Optical Materials 114 (2021) 110966

Contents lists available at ScienceDirect

Optical Materials

journal homepage: http://www.elsevier.com/locate/optmat

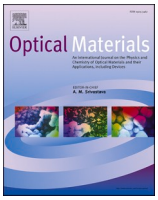

Optical and structural characteristics of electrodeposited $Cd_{1-x}Zn_xS$ nanostructured thin films

K. Erturk [a], M. Isik [b,*], M. Terlemezoglu [a,c,d], N.M. Gasanly [c]

[a] Department of Physics, Tekirdag Namik Kemal University, 59030, Tekirdag, Turkey
[b] Department of Electrical and Electronics Engineering, Atilim University, 06836, Ankara, Turkey
[c] Department of Physics, Middle East Technical University, 06800, Ankara, Turkey
[d] Center for Solar Energy Research and Applications (GÜNAM), Middle East Technical University, 06800, Ankara, Turkey

ARTICLE INFO

Keywords:
CdS
Thin film
Optical properties
$Cd_{1-x}Zn_xS$

ABSTRACT

The structural and optical characteristics of $Cd_{1-x}Zn_xS$ (CdZnS) thin films grown by the electrodeposition method were investigated in the present paper. The crystalline structure of the grown CdZnS thin film was determined as cubic wurtzite due to observed diffraction peaks associated with (111) and (220) planes. Atomic compositional ratios of the constituent elements were obtained using energy dispersive spectroscopy and doping concentration of the Zn was found as 5% ($x \sim 0.05$). Scanning electron microscopy image of the studied thin film indicated that grown film is nanostructured. Raman spectra of CdS and CdZnS thin films were measured and it was seen that observed longitudinal optical modes for CdZnS present a blue-shift. Temperature-dependent band gap energy characteristics of the thin films were studied performing transmission experiments in the 10–300 K temperature range. The analyses of the recorded transmittance spectra showed that direct band gap energy of the films decreases from 2.56 eV (10 K) to 2.51 eV (300 K) with the increase of temperature. The band gap energy vs. temperature dependency was studied applying well-known Varshni optical model and various optical parameters of the films were reported according to the results of the applied model.

1. Introduction

CdS is one of the attractive members of II-VI type semiconducting compounds. The wide range of optoelectronic device applications of the compound has kept the research interest on the CdS warm. The solar cells, light emitting diodes, nonlinear optics, transistors, sensors are some of the devices in which CdS has been used for years [1–4]. CdS has been grown in various forms like single crystal, thin film, nanoparticle, nanowire. CdS exhibits two crystalline structures of cubic and hexagonal phases. The lattice constant of the cubic phase was reported as $a = 5.832$ Å while those of the hexagonal phase were obtained as $a = 4.130$ Å and $c = 6.703$ Å [5]. The direct band gap energy of the compound has been reported around 2.48 eV which is suitable especially for solar cell applications [6].

CdS compounds have been grown with various dopants like Mn, Cu, Al, Co, Gd, Ag, Pd and etc. [7–10]. The addition of dopant may improve the structural and optical characteristics of the CdS for the purpose. One of the most studied and doped elements is zinc (Zn) which forms $Cd_{1-x}Zn_xS$ compounds in a wide range of composition ($0 \leq x \leq 1$) [11]. The significance of Zn among the other dopants come due to its large optical transmittance and closer ionic radius with Cd ($r_{Zn^{2+}} \approx r_{Cd^{2+}} \approx 0.074\ nm$) [6]. The cheapness, abundance, and non-toxicity properties of the Zn are also appreciable advantages for technological applications [12]. The direct band gap energies of the prepared $Cd_{1-x}Zn_xS$ thin films were reported as increasing from 2.33 eV ($x = 0$) to 3.33 eV ($x = 1$). The remarkable shift of the band edge with composition provides the mixed compounds attractive position in optoelectronic devices. The role of the Zn substitution on nonlinear optical characteristics of the CdS was investigated and analyses showed that third-order nonlinear optical parameters of the compound improve [6].

One of the important optical parameters for compounds utilized in optoelectronic applications is band gap energy. Since temperature affects the band gap energy of the semiconducting materials, temperature-dependent band gap energy characteristics take an effective position in device fabrication. The temperature dependency of band gap energy of CdS thin films grown by thermal evaporation technique was reported in Ref. [13]. However, nanostructured $Cd_{1-x}Zn_xS$ thin films have not been investigated so far in a similar way. The present paper aims to grow

* Corresponding author.
E-mail address: mehmet.isik@atilim.edu.tr (M. Isik).

https://doi.org/10.1016/j.optmat.2021.110966
Received 19 January 2021; Received in revised form 8 February 2021; Accepted 24 February 2021
Available online 4 March 2021

nanostructured $Cd_{1-x}Zn_xS$ ($x = 0.05$) thin films by electrodeposition method and characterize its structural and temperature-tuned band gap energy properties. Since compositional dependence of nanostructured $Cd_{1-x}Zn_xS$ thin films was previously reported in the literature [14–17], temperature-dependent band gap characteristic of the $Cd_{1-x}Zn_xS$ thin films was considered only for $x = 0.05$ to give a general view about this point. Structural properties of the films were studied utilizing x-ray diffraction (XRD), energy dispersive spectroscopy (EDS) and scanning electron microscopy (SEM) methods. The crystalline structure, atomic compositional ratio and surface morphology of the nanostructured thin films were determined by applying these experimental techniques. Optical properties of the films were considered using Raman and temperature-dependent transmission measurements. The variation of the band gap energy with temperature was revealed for $Cd_{1-x}Zn_xS$ ($x = 0.05$) films and the band gap energy vs. temperature dependency was analyzed under the light of Varshni optical model.

2. Experimental details

Nanostructured CdZnS thin films were deposited by the electrodeposition technique. Thin films were cathodically electrodeposited from an aqueous electrolytic solution containing 5 mM of cadmium chloride ($CdCl_2$) powder with 99.99% purity as Cd source, 1 mM of zinc chloride ($ZnCl_2$) as zinc source, and 50 mM sodium thiosulphate ($Na_2S_2O_3$) as a sulphur source in 100 ml of deionized water. All the chemicals were laboratory reagent grade purchased from Sigma-Aldrich. Dilute sulfuric acid (H_2SO_4) and sodium hydroxide (NaOH) were used for pH adjustment in solutions. The pH of the deposition electrolyte was adjusted to 1.5 ± 0.05. The electrolyte was heated on a magnetic stirrer heater to a temperature of 50 ± 2 °C with moderate stirring. Indium tin oxide coated glass (glass/ITO) substrates having sheet resistance of 10 Ω/sq were used for the deposition. Before deposition, all substrates were immersed in a diluted laboratory soap solution and cleaned ultrasonically for 10 min. Subsequently, these substrates were cleaned using acetone and methanol after rinsing with deionized water and finally dried in air. CdZnS deposition by electroplating was carried out using a low-cost 2-electrode system consisting of a glass/ITO working electrode as the cathode and a high purity carbon electrode as an anode immersed in an electrolyte. The electrochemical deposition was performed at a constant current of 0.6 mA for 2 h. During the deposition, the potential was observed around 1.45 V. After the deposition process, electrodeposited CdZnS thin film samples were rinsed with deionized water and then dried in air.

Deposition processes were performed in aqueous solutions using Gamry Reference 3000 Potentiostat/Galvanostat/ZRA. PHE200 Physical Electrochemistry software was used to operate the experiments. The morphology and elemental composition of deposited films were investigated by ZEISS Evo Lab6 scanning electron microscope (SEM) with EDAX detector attachment. The X-ray diffraction (XRD) pattern of samples was obtained by Rigaku miniFlex diffractometer with CuKα radiation. Raman scattering measurements were performed utilizing a Horiba-Jobin Yvon iHR550 imaging spectrometer with a three-grating monochromator and a laser with the wavelength of 532 nm used as an excitation source. The thickness of films was measured by Veeco Dektak 6 M Stylus Surface Profilometer. Temperature-dependent transmission experiments on CdZnS thin films were carried out using home-made experimental set-up which is detailed in Ref. [18]. Jenway 6400 model spectrophotometer with a resolution of 0.1 nm and accuracy of ±1 nm was used for spectroscopic measurements. The deposited thin film was placed inside Advanced Research Systems, Model CSW-202 closed cycle helium cryostat to provide the desired temperature between 10 and 300 K.

3. Results and discussions

3.1. Structural properties

The crystalline structure of the grown CdZnS thin films was determined by carrying out the XRD measurements which presented the diffraction pattern shown in Fig. 1. Both of the diffraction patterns of the ITO substrate and CdZnS/ITO structure were given in the figure. As seen CdZnS/ITO structure exhibits two additional peaks around 27.60° and 45.05° which are associated with (111) and (220) planes of cubic crystalline structure with lattice constants of $a = 5.832$ Å [5]. The presence of diffraction peaks in the XRD pattern points out that CdZnS thin films were successfully grown and have good crystallinity characteristics. Moreover, XRD pattern does not consist of peaks associated with planes of possible phases like Zn, Cd, ZnS. This may be attributed to the point of that zinc atoms occupied the lattice points and Zn-substitution does not affect the cubic crystalline structure [19].

The observed more intensive diffraction peak around 27.60° may be utilized to get information about the average crystalline size (D_{avg}) taking into consideration the following Debye Scherrer's relation [20].

$$D_{avg} = \frac{0.9\lambda}{\beta cos\theta} \tag{1}$$

where β symbolizes full-width at half maximum. When the related parameters of (111) peak were used in Eq. (1), the average crystalline size was calculated as 14.8 nm. The dislocation density (δ) and lattice strain (ε) were also estimated using the expressions [21].

$$\delta = \frac{1}{D^2} \text{ and } \varepsilon = \frac{\beta cot\theta}{4}. \tag{2}$$

The δ and ε values were calculated from these expressions as 4.6×10^{15} m^2 and 5.0×10^{-3}, respectively. The crystalline size, dislocation density and lattice strain of CdZnS nanostructured thin films for the composition of $x = 0.05$ were previously reported as 16.7 nm, 3.9×10^{15} m^2 and 7.4×10^{-3}, respectively [1]. Taking into account the differences between growth processes and physical properties of grown thin films, it may be considered that the determined values show good consistency with previously reported ones.

3.2. Surface morphology and elemental composition

The atomic compositional ratio of constituent elements was determined by performing EDS measurements. Fig. 2 shows the EDS spectrum

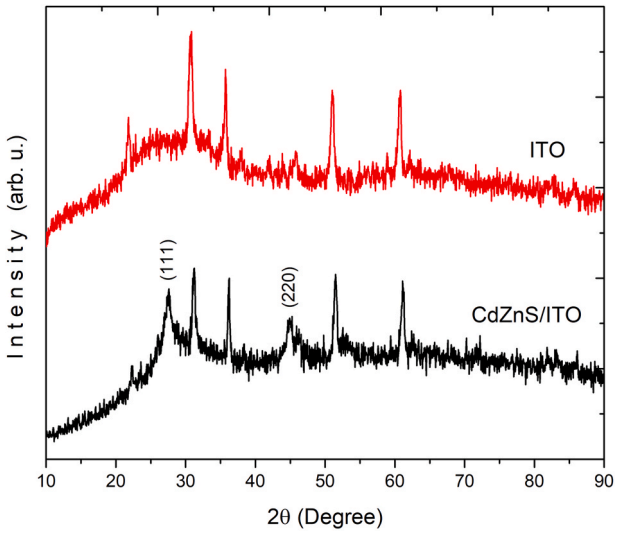

Fig. 1. XRD patterns of ITO substrate and CdZnS/ITO thin film structure.

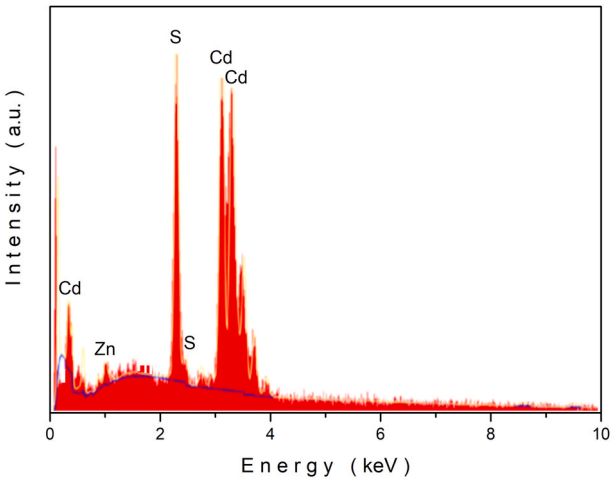

Fig. 2. EDS spectrum of CdZnS thin films.

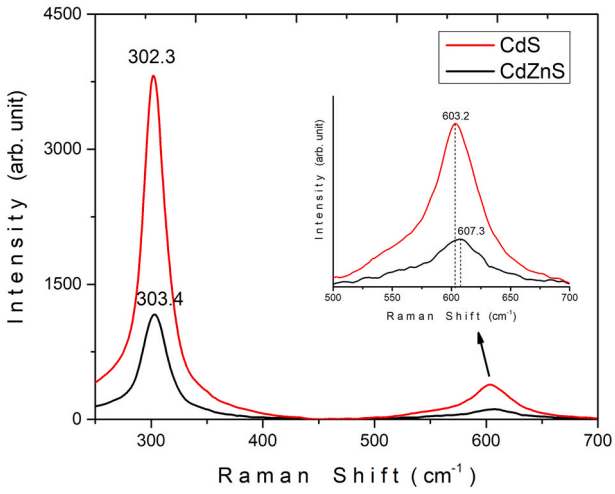

Fig. 4. Raman spectra of CdS and CdZnS thin films.

of the CdZnS thin films. As seen, the spectrum presents peaks at characteristics emission energies related with each element. The emission energies for Cd, Zn and S elements are (23.174, 22.984, 26.096, 3.134, 3.127, 3.317, 3.528, 3.717 and 0.404 keV), (8.639, 8.616, 9.572, 1.012 and 1.035 keV) and (0.163, 0.164, 2.307, 2.464 and 2.470 keV), respectively [22]. The analyses of the spectrum resulted in atomic compositional ratio (Cd: Zn: S) of (49.4 : 5.3: 45.3). This compositional ratio is well-suited with composition of $x = 0.05$ for $Cd_{1-x}Zn_xS$.

The surface morphology of the grown nanostructured thin films was studied by recording SEM image which is indicated in Fig. 3. It is seen from the SEM image that grown CdZnS thin films are nanostructured and there exist an ignorable number of pin holes and cracks over the surface. The grown thin film has been observed as uniform and dense which may be associated with well-nanostructured form.

3.3. Optical properties

Raman and temperature-dependent transmittance spectra of CdZnS nanostructured thin films were measured for optical characterization. Fig. 4 represents the Raman spectra of pure CdS and electrodeposited CdZnS thin films. Two each mode around 302.3 and 603.2 cm^{-1} for CdS, 303.4 and 607.3 cm^{-1} for CdZnS structures were observed in the spectra. The first peak is associated with longitudinal optical (LO) mode while the second peak is related to the first overtone of this LO mode [23]. When the modes of CdS and CdZnS thin films were compared, a blue-shift is seen for CdZnS. A similar shift was also reported previously [24] and this blue-shift of the observed LO modes was associated with enhancement of substitution disorder, structural fluctuations and phonon confinement [25].

Temperature-dependent transmission experiments were performed in the 10–300 K temperature and 425–900 nm spectral ranges. The room temperature spectrum is indicated in the inset of Fig. 5 in the whole applied region while temperature-dependent transmittance spectra are presented in the strong absorption region (450–550 nm) in Fig. 5. The sharp decrease of transmission below 550 nm is associated with the strong absorption of the photon energy in this region. The decrease of temperature from 300 to 10 K results in shift of the spectrum to lower wavelengths (higher energies). This behavior is well-consistent with theoretical expectations pointing out that band gap energy of the semiconducting materials increases with decrease of temperature [26]. This behavior was explained as follows: When the temperature is raised, vibrational energy of the atoms increases and so the distance between the atoms increases. The band structure of the semiconducting materials is considered taking into account the assumption of that electrons in the crystal lattice are subjected to periodic potential. The potential well of the electrons decreases due to the increase of distance between atoms. Consequently, band gap energy of the semiconductors decreases with increase in temperature. The band gap energy of the CdZnS nanostructured thin films was found performing the analyses according to Tauc expression and derivative spectroscopy technique. The absorption

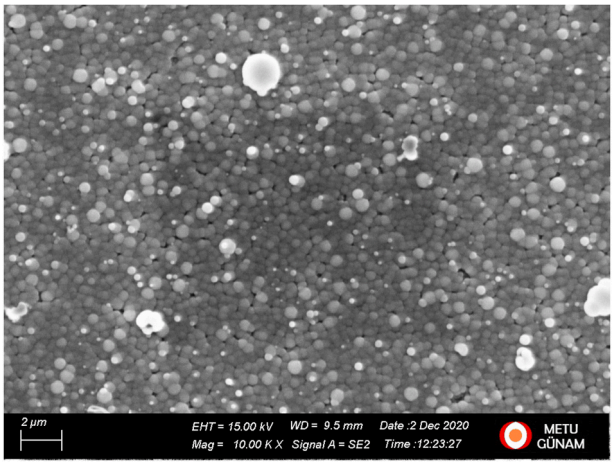

Fig. 3. SEM image of the CdZnS thin films.

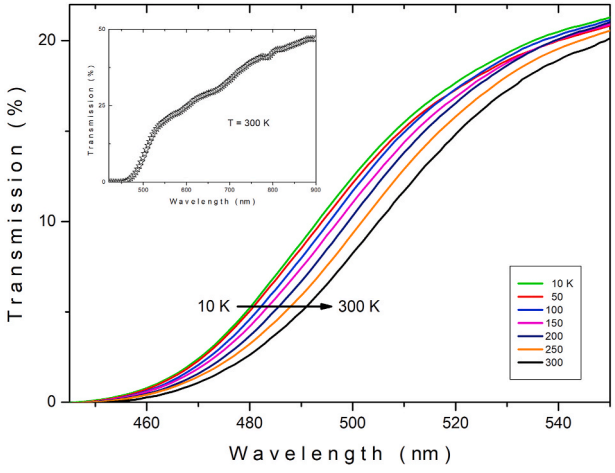

Fig. 5. Temperature-dependent transmittance spectra of CdZnS nanostructured thin films around strong absorption region. Inset indicates the room temperature spectrum in whole applied spectral range.

coefficient (α) was determined using the relation of $\alpha = -\ln(T)/d$, where d is the film thickness which was measured as $d \approx 400$ nm using Dektak 6 M profilometer. Optical band gap energy (E_g) and absorption coefficient are related by following Tauc expression [26].

$$(\alpha h\nu) = A\left(h\nu - E_g\right)^p \tag{3}$$

where A and p symbolize for band tailing parameter and index, respectively. The p index is 2 for indirect and 1/2 for direct band gap energy characteristics. The plot of $(\alpha h\nu)^{1/p}$ vs. $(h\nu)$ presents linear region around the strong absorption range. The intercept point of linear fitted line on energy axis is equal to E_g. Fig. 6 shows the related plots drawn for the more suitable index of $p = 1/2$ index. As observed from the plot, the absorption edge shifts to higher energies as the temperature was decreased. Inset of Fig. 6 was given to indicate the linear fitted process and intersection point on energy axis for room temperature data. The room temperature band gap energy ($E_{g,room}$) was obtained from the plot as 2.51 eV. This energy value increased to 2.55(5) eV when the sample temperature was 10 K. It would be worthwhile to discuss revealed room temperature gap energy considering the previously reported energies for CdS and $Cd_{1-x}Zn_xS$ compounds. $E_{g,room}$ of CdS thin films was reported around 2.39 eV [13]. The optical characterization analyses of $Cd_{1-x}Zn_xS$ nanostructured thin films for $x = 0.05$ resulted in band gap energy of 2.50 eV [1] and 2.57 eV [6]. The band gap energies of CdS films were also obtained for film thicknesses of 450, 600 and 700 nm [27]. It was observed that band gap energy decreases slightly from 2.45 to 2.42 eV when the film thickness was increased from 450 to 700 nm. The thickness of studied film in the present work is around 400 nm and when reported gap energy (2.45 eV) of 450 nm thick film was considered, there exist theoretically reasonable increase in value due to doping of zinc atoms. As seen, Zn-doping increases the band gap energy as expected. Already, band gap energy of the ZnS was found around 3.92 eV from the analyses of transmittance spectrum [28]. If the band gap energies of CdS and ZnS were compared, a remarkable difference between gap energies is seen. This band gap energy difference may be explained as follows: *Zn* ion is smaller than *Cd* ion and it is a well-known behavior for mixed compounds that the increasing concentration of smaller cation or anion results in increase in band gap energy. This point was also previously observed in literature for various mixed structures like GaS_xSe_{1-x} [29], $Cd_{1-x}Zn_xS$ [11] and $Al_xGa_{1-x}N$ [30].

As a supportive analysis method, derivative spectroscopy (DS) technique was applied to get band gap energy by plotting the spectrum of first-wavelength derivative of transmittance ($dT/d\lambda$). According to DS method, derivative of transmittance and/or reflectance present peak at energies corresponding to band gap energy [31–35]. Fig. 7 represents the spectral dependencies of $dT/d\lambda$ for some of the experimental data.

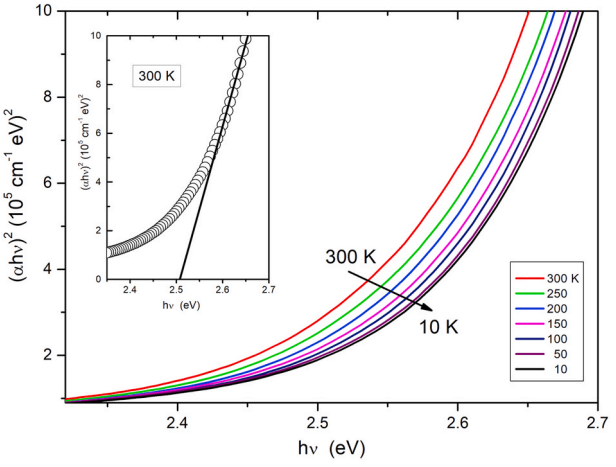

Fig. 6. Photon energy dependencies of $(\alpha h\nu)^2$ at different temperatures. Inset presents the room temperature analyses according to Tauc expression.

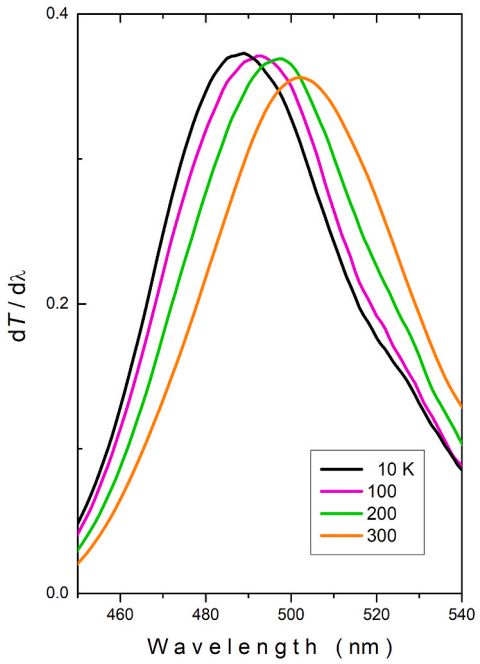

Fig. 7. $dT/d\lambda$ plots for CdZnS nanostructured thin films.

All derivative plots were not drawn to present readers more understandable/readable figure. As seen from the figure, derivative plots exhibit well-structured peaks which shift to lower wavelengths with decrease of temperature as consistent with theoretical expectations and temperature-dependent transmittance spectra given in Fig. 5. The peak for room temperature experimental data reaches its maximum intensity at $\lambda = 502$ nm which corresponds to $E_{g,room} = 2.47$ eV. The determined band gap energies from absorption coefficient and DS analyses techniques are in good consistency with each other. The band gap energy for lowest applied temperature of 10 K was found from the DS method as 2.54 eV.

The band gap energy vs. temperature dependency has been studied under the light of various models. In the present study $E_g - T$ dependency for CdZnS nanostructured thin films was investigated using the most well-known and applied following Varshni expression [36].

$$E_g(T) = E_g(0) + \frac{\gamma T^2}{T + \beta} \tag{4}$$

where E_g (0), γ and β symbolize for absolute zero temperature band gap energy, rate of change of band gap energy and Debye temperature, respectively. Fig. 8 presents $E_g - T$ dependency in which band gap energies at each temperature were determined from Tauc expression analyses. The Varshni model fitting analyses resulted in optical parameters of E_g (0) = 2.55(5) eV, $\gamma = -3.0 \times 10^{-4}$ eV/K and $\beta = 278$ K. According to Eq. (4), small variation in one of the determined band gap energies result in remarkable change in Debye temperature since β is non-dominant term in the expression. In the fitting process the error, Debye temperature was found with its tolerance as $\beta = 278 \pm 35$ K. The γ was found in the order of 10^{-4} which is the most determined order for semiconducting materials. The analyses of temperature-dependent band gap energies of CdS and ZnS were also accomplished and following optical parameters were revealed: E_g (0) = 2.41 eV, $\gamma = -1.27 \times 10^{-4}$ eV/K for CdS [13] and E_g (0) = 3.81 eV, $\gamma = -5.5 \times 10^{-4}$ eV/K for ZnS [37].

4. Conclusion

$Cd_{1-x}Zn_xS$ nanostructured thin films grown by electrodeposition method for the composition of $x \approx 0.05$ were investigated by structural

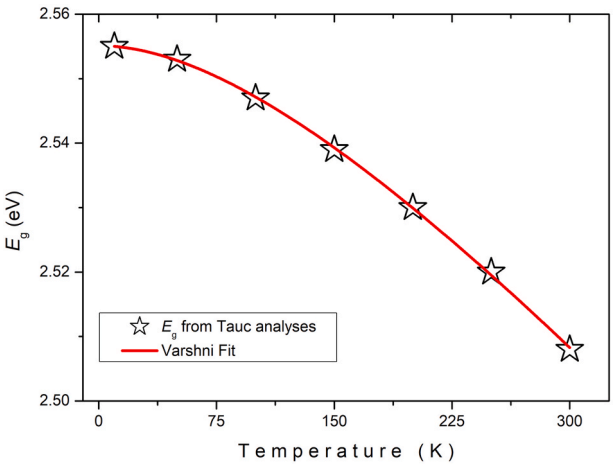

Fig. 8. Temperature-dependent band gap energy plot. Solid line indicates the fit according to Eq. (4).

and optical characterization methods. XRD pattern presented two diffraction peaks associated with (111) and (220) planes of cubic crystalline structure. SEM image of the film presented that grown thin film is well-defined nanostructured. Raman spectrum of the CdZnS thin film exhibited two peaks around 303.4 and 607.3 cm^{-1} associated with the longitudinal optical mode. It was also reported that Raman peaks of CdZnS nanostructured thin film present blue-shift compared to CdS thin film. Temperature-dependent transmittance spectra of the nanostructured films were recorded and analyses of the spectra were accomplished to get temperature variation behavior of the band gap energy. Analyses of the absorption coefficient under the light of Tauc expression resulted in room temperature band gap energy of 2.51 eV. The band gap energy increased to 2.56 eV with decrease of temperature down to 10 K. Temperature-band gap energy dependency was investigated by means of Varshni model and optical parameters of $E_g(0) = 2.55$ (5) eV, $\gamma = -3.0 \times 10^{-4}$ eV/K and $\beta = 278 \pm 35$ K were obtained as a result of successful fitting process.

CRediT authorship contribution statement

K. Erturk: Conceptualization, Resources, Investigation, Writing – original draft. **M. Isik:** Conceptualization, Investigation, Formal analysis, Methodology, Writing – original draft. **M. Terlemezoglu:** Investigation, Resources, Writing – review & editing. **N.M. Gasanly:** Supervision, Writing – review & editing.

Declaration of competing interest

The authors declare that they have no known competing financial interests or personal relationships that could have appeared to influence the work reported in this paper.

Acknowledgement

Authors gratefully acknowledge Dr. Raşit Turan and Dr. Mehmet Parlak for using their facilities to carry out the measurements in Center for Solar Energy Research and Applications (GÜNAM) in Middle East Technical University.

References

[1] M. Shkir, M. Anis, S. Shafik, M.A. Manthrammel, M.A. Sayeed, M.S. Hamdy, S. Alfaify, Physica E 118 (2020) 113955.
[2] S. Yilmaz, M. Tomakin, A. Unverdi, A. Aydin, I. Polat, E. Bacaksiz, J. Mater. Sci. Mater. Electron. 31 (2020) 12932.
[3] L.A. Gonzalez, I. Carreon-Moncada, M.A. Quevedo-Lopez, Mater. Lett. 192 (2017) 161.
[4] R.K. Sonker, B.C. Yadav, V. Gupta, M. Tomar, Mater. Chem. Phys. 239 (2020) 121975.
[5] A.A.I. Al-Bassam, A.A. Al-Juffali, A.M. Al-Dhafiri, J. Cryst. Growth 135 (1994) 476.
[6] R. Bairy, A. Jayarama, S.D. Kulkarni, M.S. Murari, H. Vijeth, Mater. Sci. Semicond. Process. 121 (2021) 105400.
[7] Z.H. Pan, S.M. Wang, R.Q. Yan, C.L. Song, Y.X. Jin, G.B. Huang, J. Huang, Opt. Mater. 109 (2020) 110324.
[8] S. Jindal, P. Sharma, J. Mater. Sci. Mater. Electron. 31 (2020) 20295.
[9] B. Poornaprakash, U. Chalapathi, P.T. Poojitha, S.V.P. Vattikuti, S.H. Park, Mater. Sci. Semicond. Process. 100 (2019) 73.
[10] S.M. Ali, M.A.M. Khan, T.S. Alkhuraiji, J. Mater. Sci. Mater. Electron. 31 (2020) 14901.
[11] S. Azizi, H.R. Dizaji, M.H. Ehsani, Optik 127 (2016) 7104.
[12] F.K. Among, J.A.M. Awudza, R.K. Nkum, F. Boakye, P.J. Thomas, P. O'Brien, Solid State Sci. 40 (2015) 50.
[13] M. Isik, H.H. Gullu, S. Delice, M. Parlak, N.M. Gasanly, Mater. Sci. Semicond. Process. 93 (2019) 148.
[14] L. Gogoi, S. Chaliha, P.K. Saikia, AIP Conf. Proc. 2100 (2019), 020034.
[15] D. Lilhare, A. Khare, Opt. Mater. 108 (2020) 110385.
[16] B. Barman, K.V. Bangera, G.K. Shivakumar, Mater. Res. Express 6 (2020) 126441.
[17] R. Zellagui, H. Dehdouh, M. Adnane, M.S. Akhtar, M.A. Saeed, Optik 207 (2020) 164377.
[18] M. Isik, H.H. Gullu, M. Parlak, N.M. Gasanly, Physica B 582 (2020) 411968.
[19] L. Ma, X. Ai, X. Wu, J. Alloys Compd. 691 (2017) 399.
[20] B.D. Cullity, S.R. Stock, Elements of X-Ray Diffraction, Prentice Hall, New Jersey, 2001.
[21] M. Birkholz, Thin Film Analysis by X-Ray Scattering, Wiley-VCH Verlag GmbH and Co. KGaA, Weinheim, 2006.
[22] J. Goldstein, D. Newbury, D. Joy, C. Lyman, P. Echlin, E. Lifshin, L. Sawyer, J. Michael, Scanning Electron Microscopy and X-Ray Microanalysis, Springer Science, LLC, New York, 2007.
[23] G.L. Song, S. Guo, X.X. Wang, Z.S. Li, B.S. Zou, H.M. Fan, R.B. Liu, New J. Phys. 17 (2015), 063024.
[24] S. Yang, J. Zhang, Appl. Phys. A 125 (2019) 454.
[25] J.R. Jayaramaiah, R. Shamanth, V. Jayanth, K.S. Shamala, Curr. Appl. Phys. 16 (2016) 799.
[26] J.I. Pankove, Optical Processes in Semiconductors, Prentice-Hall, Englewood Cliffs, New Jersey, 1971.
[27] H. Metin, R. Esen, Semicond. Sci. Technol. 18 (2003) 647.
[28] A. Attaf, A. Derbali, H. Saidi, H. Benamra, M.S. Aida, N. Attaf, H. Ezzaouia, L. Derbali, Phys. Lett. A 384 (2020) 126199.
[29] M. Isik, N.M. Gasanly, Mater. Chem. Phys. 190 (2017) 74.
[30] A. Kafi, F.D. Khodja, F. Saadaoui, S. Chibani, A. Bentayeb, M.D. Khodja, Mater. Sci. Semicond. Process. 113 (2020) 105049.
[31] L.K. Dintle, P.V.C. Luhanga, C. Moditswe, C.M. Muiva, Physica E 99 (2018) 91.
[32] D.T. Speaks, Int. J. Mech. Mater. Eng. 15 (2020) 2.
[33] M. Yilmaz, Phys. Scripta 89 (2014), 095802.
[34] Y. Caglar, M. Caglar, S. Ilican, A. Ates, J. Phys. D Appl. Phys. 42 (2009), 065421.
[35] B. Saha, K. Sarkar, A. Bera, K. Deb, R, Appl. Surf. Sci. 418 (2017) 328.
[36] Y.P. Varshni, Physica 34 (1964) 149.
[37] R. Passler, E. Griebl, H. Riepl, G. Lautner, S. Bauer, H. Preis, W. Gebhardt, B. Buda, D.J. As, D. Schikora, K. Lischka, K. Papagelis, S. Ves, J. Appl. Phys. 86 (1999) 4403.